



Study of Exclusive B Decays to Charmed Baryons at Belle

N. Gabyshev,⁸ H. Kichimi,⁸ K. Abe,⁸ K. Abe,⁴¹ T. Abe,⁴² I. Adachi,⁸ H. Aihara,⁴³
 M. Akatsu,²² Y. Asano,⁴⁸ T. Aso,⁴⁷ V. Aulchenko,¹ T. Aushev,¹² A. M. Bakich,³⁸
 E. Banas,²⁶ A. Bay,¹⁸ P. K. Behera,⁴⁹ I. Bizjak,¹³ A. Bondar,¹ A. Bozek,²⁶ M. Bračko,^{20,13}
 J. Brodzicka,²⁶ T. E. Browder,⁷ B. C. K. Casey,⁷ P. Chang,²⁵ Y. Chao,²⁵ K.-F. Chen,²⁵
 B. G. Cheon,³⁷ R. Chistov,¹² S.-K. Choi,⁶ Y. Choi,³⁷ Y. K. Choi,³⁷ M. Danilov,¹²
 L. Y. Dong,¹⁰ A. Drutskoy,¹² S. Eidelman,¹ V. Eiges,¹² Y. Enari,²² F. Fang,⁷
 A. Garmash,^{1,8} T. Gershon,⁸ B. Golob,^{19,13} J. Haba,⁸ T. Hara,³⁰ H. Hayashii,²³
 E. M. Heenan,²¹ T. Higuchi,⁴³ L. Hinz,¹⁸ T. Hojo,³⁰ T. Hokuue,²² Y. Hoshi,⁴¹ W.-S. Hou,²⁵
 H.-C. Huang,²⁵ T. Igaki,²² Y. Igarashi,⁸ T. Iijima,²² K. Inami,²² A. Ishikawa,²² R. Itoh,⁸
 H. Iwasaki,⁸ Y. Iwasaki,⁸ H. K. Jang,³⁶ J. H. Kang,⁵¹ J. S. Kang,¹⁵ P. Kapusta,²⁶
 N. Katayama,⁸ H. Kawai,² Y. Kawakami,²² T. Kawasaki,²⁸ D. W. Kim,³⁷ Heejong Kim,⁵¹
 H. J. Kim,⁵¹ H. O. Kim,³⁷ Hyunwoo Kim,¹⁵ S. K. Kim,³⁶ K. Kinoshita,⁴ S. Kobayashi,³⁴
 S. Korpar,^{20,13} P. Križan,^{19,13} P. Krokovny,¹ R. Kulasiri,⁴ Y.-J. Kwon,⁵¹ J. S. Lange,^{5,33}
 G. Leder,¹¹ S. H. Lee,³⁶ J. Li,³⁵ D. Liventsev,¹² R.-S. Lu,²⁵ J. MacNaughton,¹¹
 G. Majumder,³⁹ F. Mandl,¹¹ S. Matsumoto,³ T. Matsumoto,⁴⁵ W. Mitaroff,¹¹
 K. Miyabayashi,²³ H. Miyake,³⁰ H. Miyata,²⁸ G. R. Moloney,²¹ T. Mori,³ T. Nagamine,⁴²
 Y. Nagasaka,⁹ T. Nakadaira,⁴³ E. Nakano,²⁹ M. Nakao,⁸ H. Nakazawa,³ J. W. Nam,³⁷
 Z. Natkaniec,²⁶ S. Nishida,¹⁶ O. Nitoh,⁴⁶ S. Noguchi,²³ S. Ogawa,⁴⁰ T. Ohshima,²²
 T. Okabe,²² S. Okuno,¹⁴ S. L. Olsen,⁷ H. Ozaki,⁸ P. Pakhlov,¹² H. Palka,²⁶ C. W. Park,¹⁵
 H. Park,¹⁷ K. S. Park,³⁷ J.-P. Perroud,¹⁸ M. Peters,⁷ L. E. Piilonen,⁵⁰ F. J. Ronga,¹⁸
 N. Root,¹ K. Rybicki,²⁶ H. Sagawa,⁸ S. Saitoh,⁸ Y. Sakai,⁸ H. Sakamoto,¹⁶ M. Satapathy,⁴⁹
 O. Schneider,¹⁸ C. Schwanda,^{8,11} A. Schwartz,⁴ S. Semenov,¹² K. Senyo,²² R. Seuster,⁷
 M. E. Sevior,²¹ H. Shibuya,⁴⁰ B. Shwartz,¹ V. Sidorov,¹ N. Soni,³¹ S. Stanič,^{48,*}
 M. Starič,¹³ A. Sugi,²² A. Sugiyama,²² K. Sumisawa,⁸ T. Sumiyoshi,⁴⁵ K. Suzuki,⁸
 T. Takahashi,²⁹ F. Takasaki,⁸ N. Tamura,²⁸ J. Tanaka,⁴³ M. Tanaka,⁸ G. N. Taylor,²¹
 Y. Teramoto,²⁹ S. Tokuda,²² T. Tomura,⁴³ T. Tsuboyama,⁸ T. Tsukamoto,⁸ S. Uehara,⁸
 K. Ueno,²⁵ S. Uno,⁸ Y. Ushiroda,⁸ S. E. Vahsen,³² G. Varner,⁷ K. E. Varvell,³⁸
 C. C. Wang,²⁵ C. H. Wang,²⁴ J. G. Wang,⁵⁰ M.-Z. Wang,²⁵ Y. Watanabe,⁴⁴ E. Won,¹⁵
 B. D. Yabsley,⁵⁰ Y. Yamada,⁸ A. Yamaguchi,⁴² Y. Yamashita,²⁷ H. Yanai,²⁸ J. Yashima,⁸
 Y. Yuan,¹⁰ Y. Yusa,⁴² C. C. Zhang,¹⁰ Z. P. Zhang,³⁵ V. Zhilich,¹ and D. Žontar⁴⁸

(The Belle Collaboration)

¹*Budker Institute of Nuclear Physics, Novosibirsk*

²*Chiba University, Chiba*

³*Chuo University, Tokyo*

⁴*University of Cincinnati, Cincinnati OH*

⁵*University of Frankfurt, Frankfurt*

⁶*Gyeongsang National University, Chinju*

⁷*University of Hawaii, Honolulu HI*
⁸*High Energy Accelerator Research Organization (KEK), Tsukuba*
⁹*Hiroshima Institute of Technology, Hiroshima*
¹⁰*Institute of High Energy Physics,
Chinese Academy of Sciences, Beijing*
¹¹*Institute of High Energy Physics, Vienna*
¹²*Institute for Theoretical and Experimental Physics, Moscow*
¹³*J. Stefan Institute, Ljubljana*
¹⁴*Kanagawa University, Yokohama*
¹⁵*Korea University, Seoul*
¹⁶*Kyoto University, Kyoto*
¹⁷*Kyungpook National University, Taegu*
¹⁸*Institut de Physique des Hautes Énergies, Université de Lausanne, Lausanne*
¹⁹*University of Ljubljana, Ljubljana*
²⁰*University of Maribor, Maribor*
²¹*University of Melbourne, Victoria*
²²*Nagoya University, Nagoya*
²³*Nara Women's University, Nara*
²⁴*National Lien-Ho Institute of Technology, Miao Li*
²⁵*National Taiwan University, Taipei*
²⁶*H. Niewodniczanski Institute of Nuclear Physics, Krakow*
²⁷*Nihon Dental College, Niigata*
²⁸*Niigata University, Niigata*
²⁹*Osaka City University, Osaka*
³⁰*Osaka University, Osaka*
³¹*Panjab University, Chandigarh*
³²*Princeton University, Princeton NJ*
³³*RIKEN BNL Research Center, Brookhaven NY*
³⁴*Saga University, Saga*
³⁵*University of Science and Technology of China, Hefei*
³⁶*Seoul National University, Seoul*
³⁷*Sungkyunkwan University, Suwon*
³⁸*University of Sydney, Sydney NSW*
³⁹*Tata Institute of Fundamental Research, Bombay*
⁴⁰*Toho University, Funabashi*
⁴¹*Tohoku Gakuin University, Tagajo*
⁴²*Tohoku University, Sendai*
⁴³*University of Tokyo, Tokyo*
⁴⁴*Tokyo Institute of Technology, Tokyo*
⁴⁵*Tokyo Metropolitan University, Tokyo*
⁴⁶*Tokyo University of Agriculture and Technology, Tokyo*
⁴⁷*Toyama National College of Maritime Technology, Toyama*
⁴⁸*University of Tsukuba, Tsukuba*
⁴⁹*Utkal University, Bhubaneswar*
⁵⁰*Virginia Polytechnic Institute and State University, Blacksburg VA*
⁵¹*Yonsei University, Seoul*

(Dated: December 18, 2018)

Abstract

Using 29.1 fb^{-1} of data accumulated at the $\Upsilon(4S)$ with the Belle detector at KEKB, we have studied the decay modes $\bar{B}^0 \rightarrow \Lambda_c^+ \bar{p} \pi^+ \pi^-$, $B^- \rightarrow \Lambda_c^+ \bar{p} \pi^-$, and $\bar{B}^0 \rightarrow \Lambda_c^+ \bar{p}$. We report branching fractions of exclusive B decays to charmed baryons with four-, three- and two-body final states, including intermediate Σ_c^{++} and Σ_c^0 states. We observed $\bar{B}^0 \rightarrow \Sigma_c(2455)^{++} \bar{p} \pi^-$ for the first time with a branching fraction of $(2.38^{+0.63}_{-0.55} \pm 0.41 \pm 0.62) \times 10^{-4}$ and observed evidence for the two-body decay $B^- \rightarrow \Sigma_c(2455)^0 \bar{p}$ with a branching fraction of $(0.45^{+0.26}_{-0.19} \pm 0.07 \pm 0.12) \times 10^{-4}$. We set improved upper limits for the two-body decays $\bar{B}^0 \rightarrow \Lambda_c^+ \bar{p}$ and $\bar{B}^- \rightarrow \Sigma_c(2520)^0 \bar{p}$.

PACS numbers: 13.25.Hw, 14.20.Lq

*on leave from Nova Gorica Polytechnic, Nova Gorica

Baryon production in flavored meson decays is unique to the B meson system due to the heavy mass of the constituent b-quark. Several studies of inclusive charmed baryon production in B meson decays [1] have been made and a large branching fraction for $\bar{B} \rightarrow \Lambda_c^+ X$ of $(6.4 \pm 1.1)\%$ has been reported. However, the mechanism is not well understood. The measured inclusive Λ_c^+ momentum spectra indicate that multi-body final states are dominant in baryonic B decays. With a data sample of 2.39 fb^{-1} , CLEO [2] has studied exclusive charmed baryonic decay modes and measured the branching fractions for $\bar{B}^0 \rightarrow \Lambda_c^+ \bar{p} \pi^+ \pi^-$ and $B^- \rightarrow \Lambda_c^+ \bar{p} \pi^-$. They found no evidence for $\bar{B}^0 \rightarrow \Lambda_c^+ \bar{p}$ and provide an upper limit. So far, no observations of exclusive two-body decays or multi-body decays have been reported. On the other hand, there are theoretical predictions for branching fractions of exclusive two-body baryonic modes based on a pole model [3], a QCD sum rule [4], a diquark model [5], and a bag model [6]. The predictions of the different models vary by an order of magnitude, and experimental measurement can be used to discriminate among them. We have made a systematic study of exclusive charmed baryonic decays of \bar{B}^0 and B^- mesons into four-, three- and two-body final states including $\Sigma_c^{++/0}$ intermediate resonances, by analyzing the $\Lambda_c^+ \bar{p} \pi^+ \pi^-$, $\Lambda_c^+ \bar{p} \pi^-$ and $\Lambda_c^+ \bar{p}$ final states. Charge conjugate modes are included unless otherwise mentioned. This analysis is based on a data sample of 29.1 fb^{-1} corresponding to $3.17 \times 10^7 B\bar{B}$ pairs, accumulated at the $\Upsilon(4S)$ resonance with the Belle detector at KEKB [7].

The Belle detector is a large-solid-angle magnetic spectrometer that consists of a three-layer silicon vertex detector (SVD), a 50-layer cylindrical drift chamber (CDC), a mosaic of aerogel threshold Čerenkov counters (ACC), a barrel-like array of time-of-flight scintillation counters (TOF), and an array of CsI(Tl) crystals (ECL) located inside a superconducting solenoid coil that provides a 1.5 T magnetic field. An iron flux return located outside the coil is instrumented to detect muons and K_L mesons (KLM). The detector is described in detail elsewhere [8]. We use a GEANT based Monte Carlo (MC) simulation to model the response of the detector and determine the acceptance [9].

In searches for the decay modes $\bar{B}^0 \rightarrow \Lambda_c^+ \bar{p} \pi^+ \pi^-$, $B^- \rightarrow \Lambda_c^+ \bar{p} \pi^-$, and $\bar{B}^0 \rightarrow \Lambda_c^+ \bar{p}$, the $\Lambda_c^+ \rightarrow p K^- \pi^+$ decay mode is used. Particle identification information from the CDC dE/dx , ACC and TOF is used to provide a mass assignment for each track. A likelihood ratio $LR(A, B) = L_A/(L_A + L_B) > 0.6$ is required to identify a particle as type A , where B are the other possible assignments among π^\pm , K^\pm and $p(\bar{p})$. Electron and muon candidate tracks are removed if their probabilities from the ECL, CDC dE/dx and KLM are greater than 95%. Candidate Λ_c^+ 's are tagged if the invariant mass of the p , K^- and π^+ track combination is within $0.010 \text{ GeV}/c^2$ of the Λ_c^+ mass; tagged events are then examined for the three search modes by adding \bar{p} , π^- , and π^+ tracks. The width $\sigma_{\Lambda_c^+}$ is found to be $4.9 \text{ MeV}/c^2$, consistent with the MC.

In order to select \bar{B} meson candidates, we use the beam energy-constrained mass and energy difference, which are defined as $M_{bc} = \sqrt{E_{\text{beam}}^2 - (\sum \vec{p}_i)^2}$ and $\Delta E = \sum E_i - E_{\text{beam}}$ in the center-of-mass (CM) frame. E_{beam} is the beam energy, and E_i and \vec{p}_i are the energy and momentum vector for the i -th daughter particle of a B candidate. B candidates are selected with a loose cut to retain sideband events by requiring $M_{bc} > 5.2 \text{ GeV}/c^2$ and $|\Delta E| < 0.2 \text{ GeV}$. A vertex-constrained fit for the three daughter tracks is carried out at the Λ_c^+ vertex. For each decay mode, the virtual Λ_c^+ track and additional tracks are required to form a good vertex. If there are multiple candidates for both Λ_c^+ and B , the candidate with the minimum $\chi^2 = \chi_{\Lambda_c^+}^2 + \chi_B^2 + (M_{bc} - 5.279)^2/\sigma_{M_{bc}}^2$ is selected. Here, $\chi_{\Lambda_c^+}^2$ and χ_B^2 are the χ^2 's from the fits for the Λ_c^+ and B vertices, respectively, and $\sigma_{M_{bc}}$ is the MC value of

the M_{bc} width ($2.8 \text{ MeV}/c^2$). Loose cuts on $\chi^2_{\Lambda_c^+}$ and χ^2_B are applied to remove background from tracks arising from K_S^0 and Λ decays.

Event selection requirements are optimized using signal MC events and continuum background MC events consisting of $u\bar{u}$, $d\bar{d}$, $s\bar{s}$, and $c\bar{c}$ quark-antiquark pairs generated with the expected fractions. To suppress the continuum background, we use a Fisher discriminant constructed from 10 variables: 8 modified Fox-Wolfram moments [10], $\cos\Theta_B$, and $\cos\Theta_{\Lambda_c^+}$. Here, $\cos\Theta_B$ is the cosine of the direction of the B meson with respect to the electron beam direction, and $\cos\Theta_{\Lambda_c^+}$ is the cosine of the direction of the daughter Λ_c^+ with respect to the thrust axis of the tracks not associated with the B candidates. Both quantities are defined in the CM system. A set of 10 coefficients for each mode is optimized to maximize separation of the signal from the continuum background. The probability density functions for the signals and for the continuum, P_{sig} and P_{con} respectively, are parameterized with Gaussian functions for the three search modes and for the continuum events. A cut on the likelihood ratio $R_{\text{sfw}} = P_{\text{sig}}/(P_{\text{sig}} + P_{\text{con}}) > 0.6$ is applied to all decay modes. This cut removed 76% of the continuum background while retaining 86% of the signal for, *e.g.*, $\Lambda_c^+ \bar{p} \pi^+ \pi^-$.

Figure 1 shows the M_{bc} and ΔE distributions for the three decay modes. The M_{bc} background distributions are parameterized by the ARGUS function [11], while a Gaussian is used for the signal. The ΔE distributions are fitted with a second-order polynomial for the background and a double Gaussian for the signal. The means and widths for the M_{bc} and ΔE signals are found to be consistent with the MC values of $M_{bc} = 5.279 \text{ GeV}/c^2$, $\sigma_{M_{bc}} = 2.8 \text{ MeV}/c^2$, and $\sigma_{\Delta E} = 9.9 \text{ MeV}$. We obtain signal yields of 154^{+17}_{-16} and $38.8^{+7.6}_{-7.0}$ from the fits to the M_{bc} distributions (a) and (c), and 141^{+16}_{-15} and $30.2^{+7.0}_{-6.4}$ from the fits to the ΔE distributions (b) and (d), respectively. Here, we choose the asymmetric range of $-0.100 < \Delta E < 0.200 \text{ GeV}$ to exclude feed-down from higher multiplicity modes with extra pions; these produce the structure observed in the region $\Delta E < -0.150 \text{ GeV}$. Since M_{bc} is used in the χ^2 calculation for the best candidate selection as described previously, we use the yields resulting from the fits to the ΔE distributions to calculate branching fractions.

We observe $\bar{B}^0 \rightarrow \Lambda_c^+ \bar{p} \pi^+ \pi^-$ and $B^- \rightarrow \Lambda_c^+ \bar{p} \pi^-$ signals. For $\bar{B}^0 \rightarrow \Lambda_c^+ \bar{p}$ we find a statistical significance of only 1.9σ from a fit to a Gaussian function for the signal with mean and width fixed to those from the signal MC, and a linear background function. We thus set an upper limit of 6.1 events at the 90% confidence level based on the likelihood function, using the Bayesian method with a uniform prior. In the branching fraction calculations we use $\mathcal{B}(\Lambda_c^+ \rightarrow p K^- \pi^+) = (5.0 \pm 1.3)\%$ [12] and assume the fractions of charged and neutral B mesons to be equal.

Table I summarizes the observed yields and branching fractions. Here, the detection efficiencies are calculated assuming nonresonant decays and do not include the branching fraction for $\Lambda_c^+ \rightarrow p K^- \pi^+$. There is a common fractional error of 26% due to the uncertainty in the value of $\mathcal{B}(\Lambda_c^+ \rightarrow p K^- \pi^+)$. We include a correlated systematic error of 2% per track for tracking and particle identification. Systematics due to the $\chi^2_{\Lambda_c^+}$, χ^2_B and R_{sfw} cuts are estimated by varying cut values. The signal shape systematic error is evaluated from the variation in fit results obtained with different-order polynomials used for the background and single and double Gaussians used for the signal. The resulting total systematic errors for $\Lambda_c^+ \bar{p} \pi^+ \pi^-$, $\Lambda_c^+ \bar{p} \pi^-$ and $\Lambda_c^+ \bar{p}$ are 17.2%, 14.8% and 13.3%, respectively. Table I shows the CLEO measurements renormalized to the same $\mathcal{B}(\Lambda_c^+ \rightarrow p K^- \pi^+)$ for comparison. Our branching fraction for $\bar{B}^0 \rightarrow \Lambda_c^+ \bar{p} \pi^+ \pi^-$ is consistent with their measurement; however, our result for $B^- \rightarrow \Lambda_c^+ \bar{p} \pi^-$ is somewhat lower (1.5σ). We also set a more restrictive upper limit on $\bar{B}^0 \rightarrow \Lambda_c^+ \bar{p}$.

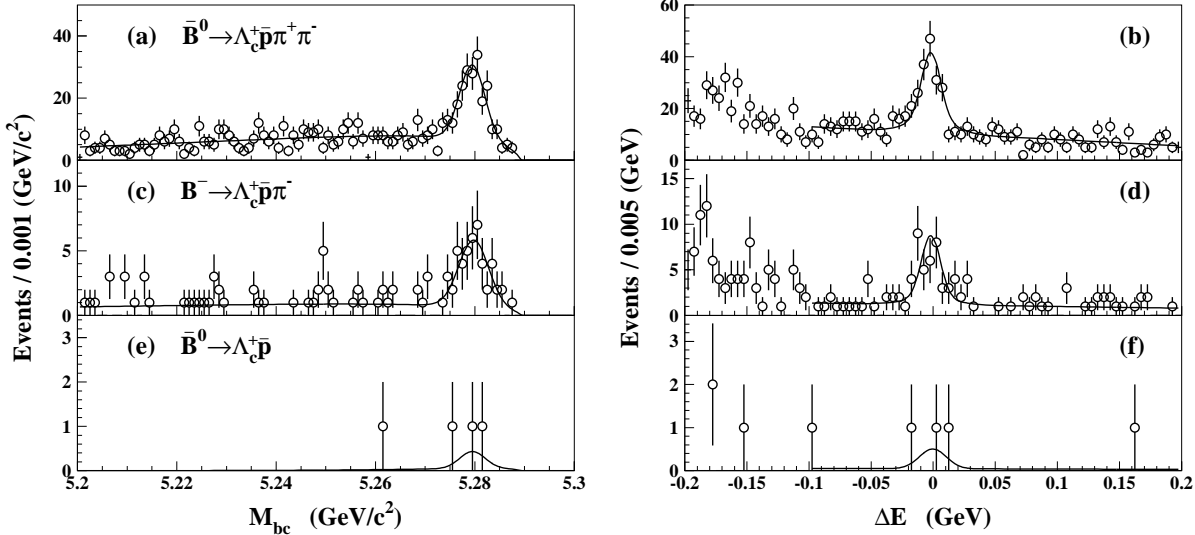


FIG. 1: M_{bc} distributions for $|\Delta E| < 0.030$ GeV and ΔE distributions for $M_{bc} > 5.270$ GeV/c^2 : (a) and (b) for $\bar{B}^0 \rightarrow \Lambda_c^+ \bar{p} \pi^+ \pi^-$, (c) and (d) for $B^- \rightarrow \Lambda_c^+ \bar{p} \pi^-$, and (e) and (f) for $\bar{B}^0 \rightarrow \Lambda_c^+ \bar{p}$. Points with errors indicate the data and the curves indicate fits (see text for details).

TABLE I: Branching fractions for $\bar{B}^0 \rightarrow \Lambda_c^+ \bar{p} \pi^+ \pi^-$, $B^- \rightarrow \Lambda_c^+ \bar{p} \pi^-$, and $\bar{B}^0 \rightarrow \Lambda_c^+ \bar{p}$. The errors are statistical, systematic, and a common error due to the uncertainty in the value of $\mathcal{B}(\Lambda_c^+ \rightarrow p K^- \pi^+)$. The CLEO results are renormalized to $\mathcal{B}(\Lambda_c^+ \rightarrow p K^- \pi^+) = (5.0 \pm 1.3)\%$ [12] for comparison.

Mode	Efficiency (%)	Yield	Significance	$\mathcal{B} (\times 10^{-4})$	CLEO ($\times 10^{-4}$)
$\bar{B}^0 \rightarrow \Lambda_c^+ \bar{p} \pi^+ \pi^-$	8.07	141^{+16}_{-15}	12.2	$11.0^{+1.2}_{-1.2} \pm 1.9 \pm 2.9$	$11.7^{+4.0}_{-3.7} \pm 2.7 \pm 3.0$
$B^- \rightarrow \Lambda_c^+ \bar{p} \pi^-$	10.2	$30.2^{+7.0}_{-6.4}$	6.0	$1.87^{+0.43}_{-0.40} \pm 0.28 \pm 0.49$	$5.5^{+2.0}_{-1.8} \pm 1.0 \pm 1.4$
$\bar{B}^0 \rightarrow \Lambda_c^+ \bar{p}$	12.9	$2.4^{+2.1}_{-1.5}$	1.9	$0.12^{+0.10}_{-0.07} \pm 0.02 \pm 0.03$	
		< 6.1 (90% CL)		< 0.31 (90% CL)	< 1.85 (90% CL)

Figure 2 shows the $\Lambda_c^+ \pi^\pm$ invariant mass distributions in the B signal region, $|\Delta E| < 0.030$ GeV and $M_{bc} > 5.270$ GeV/c^2 . Significant signals are observed for the $\Sigma_c(2455)$ and $\Sigma_c(2520)$. The shaded histograms are the normalized distributions for events in the sideband regions $-0.100 < \Delta E < -0.040$ GeV and $0.040 < \Delta E < 0.100$ GeV, which account for continuum Σ_c background. The two curves indicate the results of separate fits to the B signal and the sideband distributions, with Σ_c masses and widths fixed to fit values for the signal MC events generated with PDG values for masses and widths [12]. The background shapes are taken from a nonresonant signal MC. To extract the Σ_c yields, we performed a simultaneous likelihood fit using the B signal and sideband distributions. We express the expected number N_{Σ_c} of B events as $N_{\Sigma_c} = N_{Bb} - r \cdot N_{sb}$, where N_{Bb} is the yield in the B signal region, N_{sb} is the yield in the sideband region, and $r = 0.5$ is the normalization factor due to the ratio of their ΔE ranges, assuming a linear background shape. Table II summarizes the observed signal yields and branching fractions.

We observe the $\bar{B}^0 \rightarrow \Sigma_c(2455)^{++} \bar{p} \pi^-$ decay for the first time with a statistical significance of 5.3σ , and evidence for $\bar{B}^0 \rightarrow \Sigma_c(2520)^{++} \bar{p} \pi^-$ with a significance of 3.5σ . We observe evidence for the two-body decay $B^- \rightarrow \Sigma_c(2455)^0 \bar{p}$ with a significance of 3.0σ . We also see

less evidence for $B^- \rightarrow \Sigma_c(2520)^0 \bar{p}$ and set upper limit on the branching fraction.

Our results provide stringent constraints upon theoretical predictions [3, 4, 5, 6]. The predictions for $\bar{B}^0 \rightarrow \Lambda_c^+ \bar{p}$ in [3, 4, 5] were already much larger than the CLEO experimental upper limit [2]; here we set an even more restrictive upper limit. A recent study based on a bag model [6] gives predictions of branching fractions of $\leq (0.1 \sim 0.3) \times 10^{-4}$ for $\bar{B}^0 \rightarrow \Lambda_c^+ \bar{p}$ and $(4.3 \sim 15.1) \times 10^{-4}$ for $B^- \rightarrow \Lambda_c^+ \bar{p}\pi^-$. Our upper limit for $\bar{B}^0 \rightarrow \Lambda_c^+ \bar{p}$ does not contradict this model, while our measured result for $B^- \rightarrow \Lambda_c^+ \bar{p}\pi^-$ is much smaller than its predicted value.

In summary, we have observed the exclusive three-body decay $\bar{B}^0 \rightarrow \Sigma_c(2455)^{++} \bar{p}\pi^-$ for the first time and observed evidence for the exclusive two-body decay $B^- \rightarrow \Sigma_c(2455)^0 \bar{p}$. We make improved measurements of the branching fractions for $\bar{B}^0 \rightarrow \Lambda_c^+ \bar{p}\pi^+ \pi^-$ and $B^- \rightarrow \Lambda_c^+ \bar{p}\pi^-$, and also set a more restrictive upper limit on $\bar{B}^0 \rightarrow \Lambda_c^+ \bar{p}$.

TABLE II: Efficiencies, yields, significances and branching fractions for decay modes with $\Sigma_c^{++/0}$ resonances. The errors are statistical, systematic, and a common error due to the uncertainty in the value of $\mathcal{B}(\Lambda_c^+ \rightarrow pK^-\pi^+)$.

Mode	Efficiency (%)	Yield	Significance	$\mathcal{B} (\times 10^{-4})$
$\bar{B}^0 \rightarrow \Sigma_c(2455)^{++} \bar{p}\pi^-$	4.93	$18.6^{+4.9}_{-4.3}$	5.3	$2.38^{+0.63}_{-0.55} \pm 0.41 \pm 0.62$
$\bar{B}^0 \rightarrow \Sigma_c(2520)^{++} \bar{p}\pi^-$	6.38	$16.5^{+5.8}_{-5.2}$	3.5	$1.63^{+0.57}_{-0.51} \pm 0.28 \pm 0.42$
$\bar{B}^0 \rightarrow \Sigma_c(2455)^0 \bar{p}\pi^+$	4.80	$6.4^{+3.2}_{-2.7}$	2.6	$0.84^{+0.42}_{-0.35} \pm 0.14 \pm 0.22$
		< 11.6 (90% CL)		< 1.59 (90% CL)
$\bar{B}^0 \rightarrow \Sigma_c(2520)^0 \bar{p}\pi^+$	6.35	$4.8^{+4.5}_{-4.0}$	1.2	$0.48^{+0.45}_{-0.40} \pm 0.08 \pm 0.12$
		< 11.7 (90% CL)		< 1.21 (90% CL)
$B^- \rightarrow \Sigma_c(2455)^0 \bar{p}$	6.00	$4.3^{+2.5}_{-1.8}$	3.0	$0.45^{+0.26}_{-0.19} \pm 0.07 \pm 0.12$
		< 8.5 (90% CL)		< 0.93 (90% CL)
$B^- \rightarrow \Sigma_c(2520)^0 \bar{p}$	7.47	$1.7^{+1.8}_{-1.1}$	1.8	$0.14^{+0.15}_{-0.09} \pm 0.02 \pm 0.04$
		< 5.2 (90% CL)		< 0.46 (90% CL)

Acknowledgments

We wish to thank the KEKB accelerator group for the excellent operation of the KEKB accelerator. We acknowledge support from the Ministry of Education, Culture, Sports, Science, and Technology of Japan and the Japan Society for the Promotion of Science; the Australian Research Council and the Australian Department of Industry, Science and Resources; the National Science Foundation of China under Contract No. 10175071; the Department of Science and Technology of India; the BK21 program of the Ministry of Education of Korea and the CHEP SRC program of the Korea Science and Engineering Foundation; the Polish State Committee for Scientific Research under contract No. 2P03B 17017; the Ministry of Science and Technology of the Russian Federation; the Ministry of Education, Science and Sport of Slovenia; the National Science Council and the Ministry of

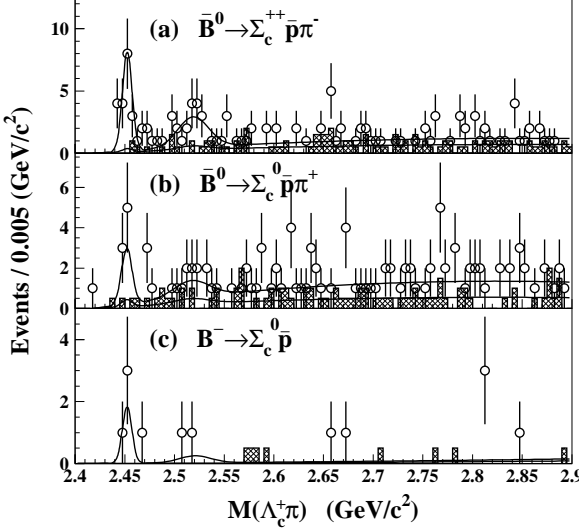


FIG. 2: Invariant mass distributions (a) $M(\Lambda_c^+ \pi^-)$ and (b) $M(\Lambda_c^+ \bar{p}\pi^+\pi^-)$, and (c) $M(\Lambda_c^+ \pi^-)$ for $\bar{B}^0 \rightarrow \Lambda_c^+ \bar{p}\pi^+\pi^-$, and $B^- \rightarrow \Lambda_c^+ \bar{p}\pi^-$. Points with errors and shaded histograms indicate data in the B signal region and normalized data in sidebands, respectively. The curves indicate fits (see text for details).

Education of Taiwan; and the U.S. Department of Energy.

[1] H. Albrecht *et al.* (ARGUS Collaboration), Phys.Lett. **B 210**, 263 (1988). G. Crawford *et al.* (CLEO Collaboration), Phys. Rev. **D 45**, 752 (1992), and M. Procaro *et al.* (CLEO Collaboration), Phys. Rev. Lett. **73**, 1472 (1994).

[2] X. Fu *et al.* (CLEO Collaboration), Phys. Rev. Lett. **79**, 3125 (1997).

[3] M. Jarfi *et al.*, Phys. Lett. **B 237**, 513 (1990); M. Jarfi *et al.*, Phys. Rev. **D 43**, 1599 (1991); N. Deshpande, J. Trampetic and A. Soni, Mod. Phys. Lett. **A 3**, 749 (1988).

[4] V. Chernyak and I. Zhitnitsky, Nucl. Phys. **B 345**, 137 (1990).

[5] P. Ball and H.G. Dosch, Z. Phys. **C 51**, 445 (1991).

[6] H. Cheng and K. Yang, Phys. Rev. **D 65**, 054028 (2002).

[7] E. Kikutani ed., KEK preprint 2001-157(2001) to appear in Nucl. Instr. Meth. **A** (2002).

[8] A. Abashian *et al.* (Belle Collaboration), Nucl. Instr. Meth. **A 479**, 117 (2002).

[9] Events are generated with the CLEO QQ program (<http://www.lns.cornell.edu/public/CLEO/soft/QQ>). The detector response is simulated using GEANT, R.Brun *et al.*, GEANT 3.21, CERN Report DD/EE/84-1, 1984.

[10] The Fox-Wolfram moments are introduced in G.C. Fox and S. Wolfram, Phys. Rev. Lett. **41**, 1581 (1978). The Fisher discriminant used by Belle is described in K. Abe *et al.* (Belle Collaboration), Phys. Rev. Lett. **87**, 101801 (2001) and K. Abe *et al.* (Belle Collaboration), Phys. Lett. **B 511**, 151 (2001).

[11] H. Albrecht *et al.* (ARGUS Collaboration), Phys. Lett. **B 229**, 304 (1989).

[12] D.E. Groom *et al.* (Particle Data Group), Eur. Phys. J. **C 15**, 636 (2000).